JOURNAL OF GUIDANCE, CONTROL, AND DYNAMICS
Vol. 19, No. 1, January–February 1996

Analysis of the Dereverberated Transfer Function in Finite Dimensions

Khoichi Matsuda* and Hironori A. Fujii†
Tokyo Metropolitan Institute of Technology, Hino, Tokyo 191, Japan

It is verified numerically that the dereverberated transfer function can be approximated with sufficient precision by making use of the model based on the reverberant transfer function with damping augmentation. In a spring-mass system, the dereverberated transfer function is derived from the equation of motion to be discontinuous in slope and to be of infinite dimensions, whereas the reverberant transfer function of finite dimensions. Another approximation is obtained to the dereverberated transfer function from the fact that the closed-loop transfer function is identical to the dereverberated transfer function when all of the reflective waves are canceled at the structural boundaries except for the location of the actuator. The dereverberated transfer function is represented as a solution of an algebraic equation with frequency-varying coefficients. The approximate solution is obtained with the help of the least-squares procedures for determining the model based on the orthogonal polynomials.

Introduction

THE dereverberated transfer function (DTF) appears in many issues on dynamics[1] and control of flexible structures, particularly in the wave-based techniques[2–8] for vibration suppression. This technique is based on the observation that the vibratory motion of flexible structures can be viewed as a superposition of traveling waves. The DTF[7] is a transfer function, ratio of an output to an input, obtained by canceling all of the reflective waves at the structural boundaries except for the actuator locations, whereas a transfer function with the reflection is termed the reverberant transfer function (RTF).[7] In a semi-infinite beam, elastic waves travel without any reflection if the inputs are applied to the only structural boundary to give a DTF as a usual input–output relation. The DTFs can be computed from the experimental data of the RTFs with the help of 1) the cepstrum of the impulse response, 2) moving averaging for the logarithmic values, and 3) parametric optimization for determining the logarithmic averaging. For further detail of the computational methods, see Refs. 7 and 8. In a simple mathematical model described by a partial differential equation, the DTF is an irrational function, and it can be related to the RTF with infinite dimensions, to be verified later, by making use of the properties of the semi-infinite beam. It is thought that the DTF can also be approximately associated with the RTF in finite dimensions. Infinite dimensional systems can be approximated to be of finite dimensions by making use of many approaches,[9–11] and they are usually analyzed as a rational function independent of the RTFs. The DTF is derived from the experimental data of the RTF through the use of the specified three methods, and no explicit relation of the DTF is obtained to the associated RTF in these cases due to lack of the utilization of the mathematical structure of the RTF. No report on structural aspects of DTFs with their relation to the RTFs encourages us to investigate it.

This paper aims to show the relation between the DTF and the RTF from three points of view. The RTF is matched to the DTF by tuning the damping factors both for the zeros and for the poles, and it is numerically verified by the least-squares procedures for fitting the model to the ideal DTF. In a spring-mass system, the DTF is analytically derived and expected to be of finite dimensions for the RTF with finite dimensions. The dereverberated system is artificially created by canceling all of the reflective waves at the structural boundaries of a flexible structure on making use of an additive controller input. For a limited class of system, the DTF is represented as a solution of an algebraic equation with frequency-varying coefficients (RTFs) that is derived from the fact that the closed-loop transfer function becomes the DTF in this case. The solution is analyzed through the use of a matrix-fraction description, and the approximate solution is given in finite dimensions by the parameter optimization technique.

Received Dec. 27, 1994; revision received June 13, 1995; accepted for publication Sept. 13, 1995.

*Graduate Student, Department of Aerospace Engineering, 6-6 Asahigaoka. Student Member AIAA.

†Professor, Department of Aerospace Engineering, 6-6 Asahigaoka. Senior Member AIAA.

Preliminaries: Characteristics of a Dereverberated Transfer Function

The characteristics of the DTF are summarized here, and the motivation is further clarified for associating the DTF with the RTF. In general, the DTF shows smooth responses on the frequency axis, and it is of infinite dimensions, that is, such irrational functions as $\sqrt{s}$ and $\exp(-Ls)$. Figure 1 compares the dereverberated and reverberated transfer functions of a flexible beam in their frequency responses. As for the magnitude of the transfer functions, the DTF is a logarithmic averaging of the RTF, and this characteristic is utilized for analysis of a complex vibrator.[1] The DTF is identical to the RTF in a semi-infinite beam in which elastic waves are generated only at the structural boundary; they travel without the reflection. This corresponds to canceling reflective waves at the boundaries for flexible structures with finite size. A shift is induced from the RTF to the DTF both by enlarging the size of a stucture and by decreasing the magnitude of the reflective waves at the structural boundaries. The RTF can be represented by a pole-zero model, and we believe that it is important to consider how poles and zeros of the RTF are

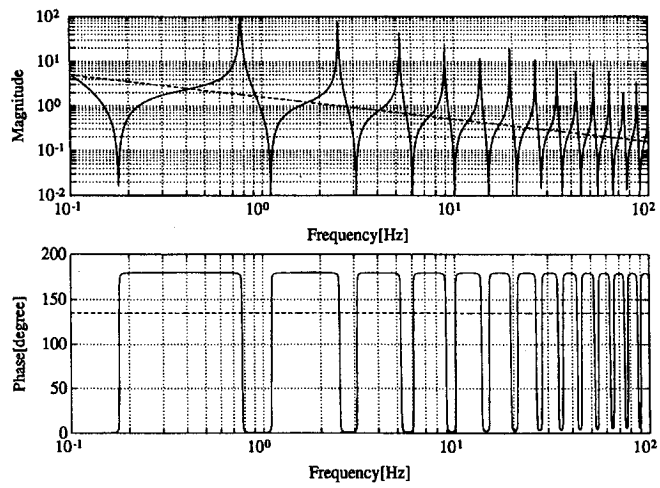

Fig. 1 Comparison between RTF (solid line) and DTF (dashed line).

shifted to those of the DTF with respect to variations both in the size of the structure and in the magnitude of the reflective waves. Of course, the DTF cannot be exactly represented by making use of the poles and zeros in a manner similar to the RTF. It is expected that an approximate representation is obtained for the DTF from a new point of view. This idea is clarified through the use of a simple example in the following.

Let us consider a flexible string with both ends being free; then the transfer function from the force input to the velocity sensor output is

$$G(s) = v/f = -\cosh s\eta/\sinh s(\eta + \xi) \tag{1}$$

where v is the velocity at $x = \xi$, f the force at the left end ($x = 0$), and η the displacement from the location of the sensor to the right end. The DTF is obtained by making the string semi-infinite in length, that is, $\eta \to \infty$ in Eq. (1) to give

$$X_0(s) = -e^{-s\xi} \tag{2}$$

The zeros of the RTF $G(s)$ are, with the help of the length parameter η,

$$z_n = \pm j\pi(n - 0.5)/\eta \qquad n = 1, 2, \ldots \tag{3}$$

It is easily understood that the zeros move to the origin on the imaginary axis in the complex plane as $\eta \to \infty$. All of the zeros are at the origin in the limit, and the same phenomenon is also observed in the case of the poles. Multiple pole-zero cancelations occur at the origin, and no insight is obtained into the pole-zero characteristics of the DTF itself in this case. In the following it is studied how poles and zeros of the RTF are moved on the complex plane through variation in the magnitude of the reflective waves.

Again, let us consider a flexible string with both ends free, and for simplicity, the sensor is collocated with the actuator at the left end. The scattering parameter is introduced to represent the ratio of the reflective wave to the incident wave at the right end of the string. The transfer function from the force input to the velocity output is written using the scattering parameter as follows:

$$G(s) = (\tau e^{-s} + e^{s})/(\tau e^{-s} - e^{s}) \tag{4}$$

where τ is the scattering parameter. It can be easily understood that the RTF $G(s)$ approaches -1, the ideal value of the DTF, at $\tau = 0$ when there is no reflective wave at the right end of the string. With the help of the denominator and numerator of Eq. (4), fundamental manipulations give variations of the poles and zeros with respect to τ.

For the poles:

$$p_n = -c \pm j\pi n \qquad n = 0, 1, 2, \ldots \tag{5}$$

and for the zeros:

$$z_n = -c \pm j\pi(n - 0.5) \qquad n = 1, 2, \ldots \tag{6}$$

where

$$c = -\ell_n\tau/2 \tag{7}$$

It is well known that a pole-zero representation of Eq. (4) can be obtained through the use of an infinite product expansion with the help of Eqs. (5) and (6). From Eqs. (5) and (6), it seems that all of the poles and zeros move to infinity at $\tau = 0$ in a direction parallel to the negative real axis. It can easily be understood from Eq. (4), however, that both the denominator and numerator become a transcendental function that has no zero at $\tau = 0$ and that both the poles and zeros should not be defined by making use of Eqs. (5) and (6) without reflective waves at the right end of the string. A complex irrational function can be well approximated by using a rational function with poles and zeros in finite magnitude for a frequency region. The variation of τ produces an effect both on the real parts of the poles and zeros and on the magnitude of the gain in this case. Trajectories of poles and zeros are not generally known with respect to τ in explicit forms, such as Eqs. (5) and (6). It is confirmed that decrease of the scattering parameter leads to damping augmentation for the poles and zeros of the RTF since it represents energy dissipation of the system with a fixed order. Taking these two facts into account, we present the idea that the RTF is matched to the associate DTF by tuning the damping factors both for the zeros and for the poles. The damping augmentation is expressed through the use of the damping factors in this case, and it is selected due to the fact that the poles and zeros of the DTF can be easily related to those of the associate RTF and that its physical meaning is obtained with the help of a second-order system.

Another motivation for introducing the previous interpretation of the DTF is due to the wave-based controller design technique for vibration suppression. This controller design technique can be roughly formulated in an optimal control setting as follows.

Given the open-loop plant

$$y = X_0(s)u + d(a) \tag{8}$$

determine a dynamic compensator

$$u = K(s)y \tag{9}$$

that minimizes the performance index

$$J = J(b, y, u) \tag{10}$$

where y are sensor outputs, u controller inputs, X_0 a DTF, a incident waves into a location of the sensor, b reflective waves at a location of the actuator, and d disturbances, a function of a. The performance indices are selected to minimize the reflective waves b in magnitude or power flow into the system. In many cases, the compensator is selected such that the incident waves have the minimal effect on the reflective waves in the closed-loop system, which can be viewed in the optimal control setting as Eqs. (8–10). The stability and performance of the closed-loop system depend both on the relation between the DTF and RTF and on the selection of the performance index. It is regarded as being an optimum among the wave-based techniques to cancel all of the reflective waves at the location of the actuator by using controller inputs. Further improvement cannot be achieved on the performance of the closed-loop system in this controller design framework. This optimal controller is derived without constraints both on the magnitude and on the bandwidth of the controller inputs. It is known that the optimal closed-loop transfer function can be interpreted as having the same poles as those of the DTF in infinite dimensions. The optimal closed-loop response can be approximately achieved by assigning the closed-loop poles to those of the DTF, employing a modal model based on the standing waves, which has been already investigated in Ref. 12. The DTF can be interpreted as the sum of the RTF and large measurement noise. It is possible to formulate the wave-based controller design using the RTF with the colored noise only if the DTF is in a parametrized form, which is under investigation.

In this paper, we put forth the simple idea that the DTF can be approximately derived from the RTF by adequately tuning all of the damping factors in the pole-zero representation. This idea is numerically verified by the employment of simple examples in the following.

Numerical Studies: Least-Squares Procedures

The DTF is approximated in a parametrized form by making use of a least-squares procedure. Here the model is not constrained with respect to its order, whereas model order and precision of approximation are usually traded off in the approximation of an irrational function. The problem is to specify how precisely it is possible to match a DTF and an associate RTF with damping augmentation. The performance index to be minimized is defined as follows:

$$J = \frac{1}{2}\sum_{n=1}^{N} E(j\omega_n)E^*(j\omega_n)\log_{10}\frac{\omega_n}{\omega_{n-1}} \tag{11}$$

where N is the number of the sampled points on the frequency axis and E^* is the complex conjugate of E. The difference is

$$E(s) = \left[X_0^a(s) - X_0(s)\right]/X_0(s) \tag{12}$$

Table 1 Results of the least-squares procedures for flexible beams

Model (beam)	r^a	Cost ($\times 10^{-4}$)	Δg^b ($\times 10^{-3}$)	Δp^c ($\times 10^{-1}$ deg)	Truncation number Ni	Nr	N
Pinned-free	0.0	6.4	8.0	4.1	800	0	800
	0.1	7.3	8.7	3.6	110	11	121
	0.5	29	17	8.4	470	200	670
	0.9	8.9	13	6.4	910	2000	2910
Free-free	0.0	18	13	6.6	700	0	700
	0.1	18	14	6.2	120	12	132
	0.5	10	12	5.8	350	350	700
	0.9	37	21	9.6	800	1900	2700
Pinned-fixed	0.0	1.6	4.9	2.7	600	0	600
	0.1	2.0	5.5	3.0	100	10	110
	0.5	7.5	8.1	4.5	390	170	560
	0.9	5.8	10	5.1	600	1400	2000

[a]Ratios of sensor locations to the beam length. [b]Means of $||X_0^a| - |X_0||/|X_0|$. [c]Means of $|\angle X_0^a - \angle X_0|$.

where X_0^a is a model of the DTF based on the RTF, to be presented later. On making use of the real and imaginary components, Eq. (11) is multiplied through by the complex conjugate to give

$$|E|^2 = 1 + \left(|X_0^a|/|X_0|\right)^2 - 2\left(|X_0^a|/|X_0|\right)\cos\left(\angle X_0^a - \angle X_0\right) \tag{13}$$

The ideal DTF takes a large dynamic range of frequency response in magnitude for a frequency region of 4 decades in which the cost is evaluated. Performance indices that include only the absolute differences assign little weight to matching the model and the ideal values in low-gain region, where the absolute difference is small in magnitude even though the relative difference is large. The ratio of model gain to the ideal gain is weighted at each frequency in the present case. The use of a logarithmic performance index[13] has been reported elsewhere.

We investigate the validity of the aforementioned idea through the use of transfer functions in an Euler–Bernoulli beam both with various sensor locations and with three pairs of boundary conditions: pinned/free, free/free, and pinned/fixed, where in each pair, the entries represent the conditions at the left and right ends of the beam in turn. An angular sensor is located between the left and right ends of each beam, and a torque actuator is fixed at the left end. The length of the beam is unity, and the sensor is located at one of four points: $r = 0.0, 0.1, 0.5$, or 0.9. The optimal solutions are computed by making use of a nonlinear optimization technique, the conjugate-gradient method, using the Polak–Ribiere–Polyak formula for modification of the searching direction and the golden section method for line search. On making use of an infinite-product expansion, the RTF can be written as

$$G(s) = k\left\{\prod_{n=1}^{Nr}\left[1 - \left(\frac{s}{e_n}\right)^2\right] \times \prod_{n=1}^{Ni}\left[1 + \left(\frac{s}{b_n}\right)^2\right] \Big/ s^2\prod_{n=1}^{N}\left[1 + \left(\frac{s}{a_n}\right)^2\right]\right\} \tag{14}$$

when the solution DTF becomes

$$X_0(s) = ke^2\left\{\prod_{n=1}^{Nr}\left[1 - \left(\frac{s}{\hat{e}_n}\right)^2\right] \times \prod_{n=1}^{Ni}\left[1 + 2d_n\frac{s}{b_n} + \left(\frac{s}{b_n}\right)^2\right] \Big/ (s^2 + 2\alpha\beta^2 s + \beta^4) \times \prod_{n=1}^{N}\left[1 + 2c_n\frac{s}{a_n} + \left(\frac{s}{a_n}\right)^2\right]\right\} \tag{15}$$

where the truncation number $N = Nr + Ni$; the shifts of the poles at the origin, α and β, and the damping factors, c_n and d_n, are determined so as to agree with the ideal DTF; and the real zeros $\hat{e}_n$ are the same as those of the ideal DTF that are always derived analytically in the present cases. The bending rigidity, the mass per unit length, and the beam length are all unity, which corresponds to an Euler–Bernoulli beam in dimensionless form. A pair of real zeros of the RTF scarcely move on the real axis, preserving the symmetrical locations when the RTF is shifted to the DTF except for the case where the sensor is located at the right end since they are nearly a function of the displacement between the locations of the actuator and sensor.[14] It is known that better agreement of the real zeros is obtained for the higher frequency region between the RTF and DTF. Note that the DTFs are the same over the two pairs of the boundary conditions: pinned/free and pinned/fixed, because the DTF is dependent only on the structural properties between the locations of the sensor and actuator. Pole-zero cancelations occur at the origin in a product expansion of the RTF in the pinned-fixed case. This phenomenon is not necessarily unchanged under the shift from the RTF to the DTF, and new parameters γ and η are introduced to represent the shifts of the zeros at the origin in the same manner as that of the poles in Eq. (15), where γ is the damping factor and η the squared root of frequency. The number of the real zeros, however could not be in agreement with the ideal value according to the sensor locations, that is, a pair of real zeros could be missing nearest the origin in the model. Then the zeros should be shifted from the origin onto the real axis, and the parameters γ and η are not necessary in this case.

Table 2 Optimal parameters (I)

Model (beam)	r	e	α	β	c_1	d_1	d_2
Pinned-free	0.0	1.0	2.0	1.1	1.4	1.4	——
	0.1	0.91	1.9	1.1	1.0	1.5	1.3
	0.5	1.2	2.5	1.3	1.2	1.3	2.2
	0.9	0.40	1.6	0.74	1.1	16	11
Free-free	0.0	1.0	2.3	1.4	1.6	1.6	——
	0.1	0.87	2.1	1.3	1.2	1.7	1.5
	0.5	0.58	1.9	1.1	1.0	5.9	2.6
	0.9	0.89	2.5	1.4	1.2	12	31
Pinned-fixed	0.0	1.0	1.7	0.82	1.1	1.1	——
	0.1	0.98	1.8	0.83	0.91	1.1	1.3
	0.5	0.93	1.9	0.93	2.1	6.2	4.6
	0.9	2.2	1.7	0.73	1.2	16	28

Tables 1–3 summarize results of the least-squares procedures for flexible beams. The performance index is evaluated by using the differences of the model from the ideal at 50 points on the frequency axis, determined by confirming the two digits of precision in the values of the cost after the trials for a few cases. The sampled points are distributed with equal logarithmic spacing over a frequency region of four decades from 10^{-1} to 10^3 Hz, in which there are about 25 flexible modes for each RTF. The approximate DTFs deviate from the ideal ones both by the magnitude of order 10^{-2} and by the phase of order 10^{-2} deg over all of the cases, as shown in Table 1. These results should be evaluated by taking into account the fact that for

Table 3 Optimal parameters (II)

Model (beam)	r	d_3	d_4	d_5	d_6	d_7	γ	η
Pinned-free	0.1	1.5	1.2	1.3	1.1	1.2	——	——
	0.5	2.6	3.1	3.4	2.9	2.5	——	——
	0.9	25	22	29	——	——	——	——
Free-free	0.1	1.5	1.2	1.5	1.8	1.3	——	——
	0.5	2.6	3.1	3.4	2.9	2.5	——	——
	0.9	27	23	31	——	——	——	——
Pinned-fixed	0.0	——	——	——	——	——	1.4	1.0
	0.1	1.1	1.1	1.0	1.0	1.0	1.6	0.98
	0.5	4.4	4.6	6.3	8.1	5.2	——	——
	0.9	26	28	25	34	31	——	——

the DTFs the magnitude is of order 10^{-2} minimum, the phase of order 10^3 deg maximum, and the truncation number of order 10^3 maximum. We conclude that the DTF can be approximated with sufficient precision by making use of the parametrizations based on the RTF, although in practice a lower order model would be obtained for the DTF with the same precision by other techniques. Each optimization process is considered to have converged whenever the root mean square of the gradient vector and the variation of the parameters to be determined are less than 10^{-6} and 10^{-9}, respectively. If there is the minimum value of the cost, the optimal truncation numbers Nr and Ni are searched within the two digit of the precision of the cost value and if not, they are determined such that the cost is unchanged with the same precision.

It is not natural that the damping factors c_n or d_n are different over all of the flexible modes in Eq. (15) because the damping factor is dimensionless and the present system is of a significantly large number of dimensions. Thus, we select an approach to determin the optimal damping factors of the zeros in Eq. (15). The number of parameters is unity at first, that is, the damping factors are the same over all of the zeros and increases such that a damping factor becomes independent, in turn, from the first flexible mode according to the convergency of the cost. The final damping factor is the same over all of the residual flexible modes in Tables 2 and 3. For the poles, all of the damping factors are assumed to be the same, based on the fact that under the assumption the DTF is approximated with sufficient precision when the sensor is collocated at the actuator and that locations of the poles are independent of that of the sensor on the beam, which is almost satisfied as shown in Table 2. The poles and zeros of the DTFs are considered to be at the real axis in the complex plane from the values of the optimal damping factors in Tables 2 and 3. For the truncation of the models, the effect is larger as the sensor is located farther from the position of the actuator. Figure 2 shows a comparison between the approximate and ideal DTFs for the free-free flexible beam at $r = 0.9$ when the performance index is at the worst values over all of the cases in the least-square procedures, as shown in Table 1. The deviation is relatively larger at the neighborhood of the origin. All of the ideal DTFs have an essential singular point at the origin of the complex plane in the present case. At the singular point, it is difficult to represent features of the ideal exactly as those of the system with finite dimensions due to the definition of the singularity. The DTF is experimentally determined from data of the open-loop plant, and it is identified with its model by the least-squares procedures so as to minimize the performance index[8]

$$J = \frac{1}{2}\sum_{n=1}^{N}\left|\ell_n\left[X_0^a(j\omega_n)\right] - \ell_n\left[G^e(j\omega_n)\right]\right|^2 \log_{10}\frac{\omega_n}{\omega_{n-1}} \qquad (16)$$

where G^e denotes the frequency response data of the open-loop plant and the difference E is multiplied through by the complex conjugate to give

$$|E|^2 = \left[\ell_n\left(\left|X_0^a\right|/\left|G^e\right|\right)\right]^2 + \left(\angle X_0^a - \angle G^e\right)^2 \qquad (17)$$

The selection of the difference in Eq. (16) is based on schematic comparisons of DTFs with the associate RTFs, as shown in Fig. 1. The DTF can be regarded as the mean values of the RTF, both for the logarithmic values in magnitude and for the absolute values in phase to give Eq. (17) for the cost at each sampled point. The initial guess can be obtained for each parameter of the model of the DTF from the optimal values in Tables 2 and 3.

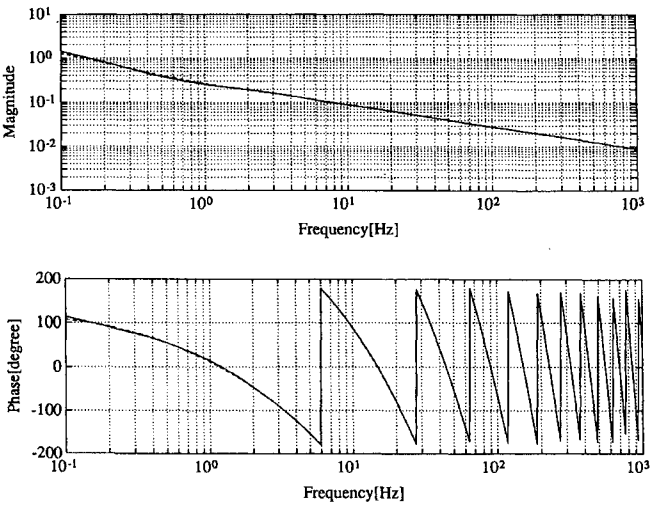

Fig. 2 Comparison of the approximate DTF (solid line) with the ideal (dashed line) for free-free beam with $r = 0.9$.

Dereverberated Transfer Function in a Spring-Mass System

The DTF is analyzed by employing a spring-mass system in place of the distributed parameter systems. It is expected that the DTF is expressed mathematically with finite dimensions in this case. Let us consider a simple spring-mass system consisting of N identical masses and $(N-1)$ identical interconnecting springs with the boundary condition being indeterminate at the right end. The equation of motion with respect to each point mass is

$$m\frac{d^2y_n}{dt^2} = k(y_{n+1} + y_{n-1} - 2y_n) \qquad n = 2, \ldots, N-1 \quad (18)$$

with the boundary condition at the left end

$$m\frac{d^2y_1}{dt^2} = k(y_2 - y_1) + f \qquad (19)$$

where m, k, and y denote mass, spring constant, and displacement of each point mass and f is a force input into the system. We first separate the time and spatial parts by substituting

$$y_n = A(t)e^{i\lambda n}$$

into Eq. (18) to give

$$m\ddot{A} = 2kA(\cos\lambda - 1) \qquad (20)$$

where λ is a propagation number. Equation (20) is Fourier transformed and divided by A to give a dispersion relation

$$\omega^2 = (2k/m)(1 - \cos\lambda) \qquad (21)$$

If $\lambda = \alpha + i\beta$, Eq. (21) becomes

$$\omega^2 = (2k/m)(1 - \cos\alpha\cosh\beta + i\sin\alpha\sinh\beta) \qquad (22)$$

This results in

$$\omega^2 = (2k/m)(1 - \cos\alpha\cosh\beta) \quad \text{and} \quad \sin\alpha\sinh\beta = 0 \qquad (23)$$

Thus we obtain

$$\lambda(\omega) = 2\sin^{-1}(\omega/\omega_c) \qquad \omega \le \omega_c \qquad (24)$$

and

$$\lambda(\omega) = \pi - 2i\sinh^{-1}\sqrt{(\omega/\omega_c)^2 - 1} \qquad \omega > \omega_c \qquad (25)$$

Table 4 Results of least squares procedure for a spring-mass system

n	Cost ($\times 10^3$)	$\Delta g^a(\times 10^2)$	Δp^b, deg	α	β	c_1	c_2	c_3	c_4	d_1	d_2	d_3	d_4	e
1	2.0	1.2	0.90	6.9	0.085	1.2	0.75	0.22	1.4	1.4	1.3	0.32	1.2	1.0
2	2.3	2.1	1.2	6.2	0.088	0.64	0.19	0.12	0.057	1.2	0.27	0.12	—	0.99
3	7.6	3.6	2.1	6.2	0.086	0.62	0.24	0.084	0.047	1.4	0.17	—	—	0.97
4	26	6.7	3.9	4.6	0.10	0.31	0.20	0.11	0.028	0.94	—	—	—	0.99
5	82	10	7.9	5.3	−0.10	0.28	0.096	0.035	0.0080	—	—	—	—	1.1

[a]Means of $||X_0^a| - |X_0||/|X_0|$. [b]Means of $|\angle X_0^a - \angle X_0|$.

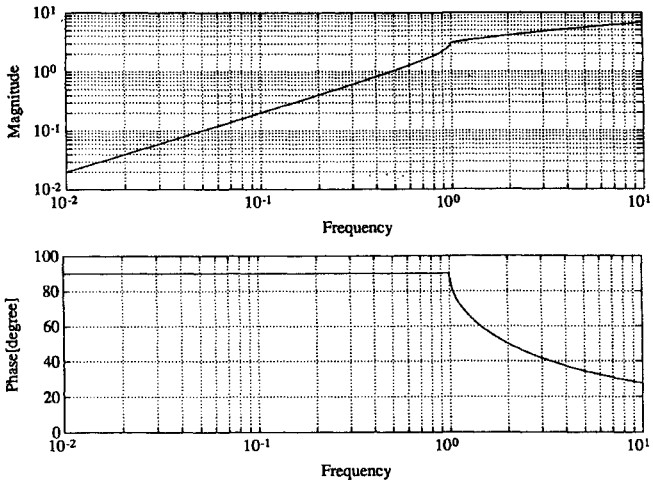

Fig. 3 Propagation number in a spring-mass system, $\omega_c = 1$.

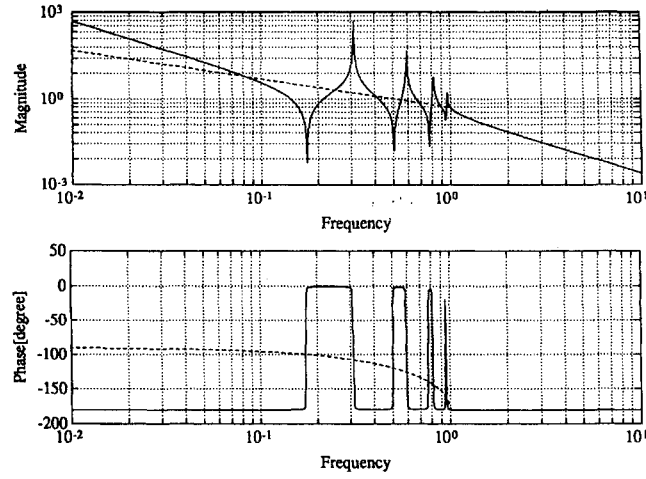

Fig. 4 Comparison between the RTF (solid line) and DTF (dashed line) for a spring-mass system, $\omega_c = 1$ and $n = 1$.

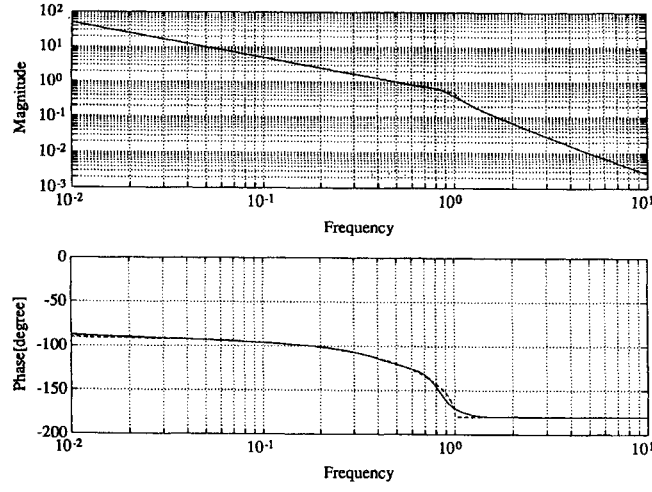

Fig. 5 Comparison of the approximate DTF (solid line) with the ideal (dashed line) for a spring-mass system, $\omega_c = 1$ and $n = 1$.

where $\omega_c = \sqrt{(4k/m)}$ is termed a cutoff frequency, and the real part of λ is uniquely determined in Eq. (25) by the requirement that λ be continuous at $\omega = \omega_c$. At the cutoff frequency, each point mass moves with inverse sign to the next point mass, that is, $y(n, t) = A(t)e^{j\pi n}$, to give the upper limit of wavelength in this system. For simplicity, m and k are assumed to be such that ω_c is unity in the following. The transfer function of λ is shown in Fig. 3, and the slopes are discontinuous both in magnitude and in phase at the cutoff frequency. The response is nearly the same as that of the propagation number in a string, $\lambda(\omega) = \omega$ for a frequency region less than the cutoff frequency. If now we make use of the propagation number λ in Eqs. (24) and (25), the displacement of each mass can be written as

$$y_n = ae^{i\lambda(n-1)} + be^{-i\lambda(n-1)} \tag{26}$$

where the first and second terms in Eq. (26) represent waves traveling to the left and right ends, respectively. Equation (19) can be rewritten with the help of Eq. (26) to give the scattering relation at the left end:

$$b(\omega) = -[(e^{j\lambda} + 4\omega^2 - 1)/(e^{-j\lambda} + 4\omega^2 - 1)]$$
$$\times a(\omega) - f(\omega)/(e^{-j\lambda} + 4\omega^2 - 1) \tag{27}$$

The DTF is derived by substituting Eq. (27) into Eq. (26) and taking account of the fact that an RTF is identical to the associate DTF when there is no incident wave at the left end,

$$X_0(\omega) = y_n/f = -e^{-i\lambda(n-1)}/(e^{-j\lambda} + 4\omega^2 - 1) \tag{28}$$

It is shown that the DTF is of infinite dimensions, whereas the RTF of finite dimensions.

Let us consider the spring-mass system with both ends being free, consisting of five masses and four springs, that is, $N = 5$. Figure 4 compares the RTF and the DTF at $n = 1$, and it is shown that the slopes are also discontinuous at the cutoff frequency both in magnitude and in phase of the DTF due to the discontinuous slope of the propagation number. Least-squares approximations are also obtained for the DTFs of Eq. (28) in the same manner as those of the distributed parameter system. The effect of the truncation number does not appear in the present system. The performance index is computed from the summation of the differences over more sampled points, $N = 600$, than that of the preceding section since the sharp response becomes relatively dominant as the optimal approximation of the DTF, particularly at $n = 5$. The results are summarized in Table 4, and only for the case $n = 1$, the optimal approximation of the DTF is compared with the ideal in Fig. 5. As a whole, these results are inferior to those of the preceding section as seen from comparison of Table 1 with Table 4. The disagreement between the ideal and approximate DTFs is larger as the sensor is located farther from the actuator, that is, as n is larger. It is considered that Eq. (15) is not suitable to the model of the DTF in the present case due to the discontinuity of the ideal. The number of the zeros decreases as n becomes larger, and particularly, the RTF has no zero when the sensor is located at the right end. From the point of view of model fitting, decreasing the degrees of freedom, the number of the model parameters, leads to increasing the cost, which cannot be observed in distributed parameter systems. It is different from dispersive systems of the preceding section in that there is no real zero in the RTF

and in that the slope of the ideal DTF is discontinuous at the cutoff frequency in the present system.

Dereverberated Transfer Function in the Closed-Loop System

In this section, we present an approach to deriving a DTF from the fact that the dereverberated system is obtained when there is no reflective wave at the structural boundaries. Another representation of a DTF is given by this approach, more specifically regarding the relation to the RTF than that of the preceding section given by Eq. (15), although the system to be investigated is less general. Artificial controller inputs are added into the system in addition to an inherent input–output relation so as to cancel all of the reflected waves at the boundaries, which leads to creation of the dereverberated system on the flexible structure. Under the assumptions of the system to be stated in the following, the relation between the RTF and DTF is expressed in a second-order algebraic equation with frequency-varying coefficients.

Formulation of an Algebraic Equation

A flexible beam or string is employed with the same boundary conditions at both ends, and two pairs of sensors and actuators are located at the symmetrical locations about the center of the length (Fig. 6). An inherent input-output pair is located on the left side at which the RTF is shifted to the associate DTF by the artificial inputs and outputs located on the right side so as to cancel all of the reflective waves. Without loss of generality, it is assumed that two pairs of collocated rate-sensors/actuators are located at both of the free ends. It is confirmed that the following argument can be applied without modification to nonminimum phase systems over a wide variety of boundary conditions. Velocity sensors and force actuators are used in the string case, whereas velocity and angular-rate sensors and torque and force actuators are located at both ends of the flexible beam. The RTF becomes the DTF when a compensator is designed for the artificial inputs so as to cancel all of the waves reflected into the left. The transfer function of the compensator is the same as the DTF at the left end, due to the boundary conditions being the same at both ends; this relation also holds in the case when the sensors are dislocated at the actuators. An algebraic equation is derived by using the fact that the closed-loop transfer functions are identical to the DTF from the controller inputs to the sensor outputs at the left end in this system. A flexible beam is employed to exemplify this approach in the following.

Flexible Beam Example

This system is governed by the equation of motion in the complex Laplace s domain as follows:

$$\frac{d^4 w}{dx^4} - s^2 w = 0 \tag{29}$$

where w denotes the transverse deflection of the beam; the bending rigidity, the mass per unit length, and the beam length are all unity. We introduce the following notation: $\dot{w} = sw$, $\dot{\theta} = s\,dw/dx$, $M = d^2w/dx^2$, and $F = d^3w/dx^3$. The standard calculation using a homogeneous solution to Eq. (29) gives the input–output relations at both ends of the beam,

$$y_0 = G_{00}u_0 + G_{01}u_1 \tag{30}$$

$$y_1 = G_{10}u_0 + G_{11}u_1 \tag{31}$$

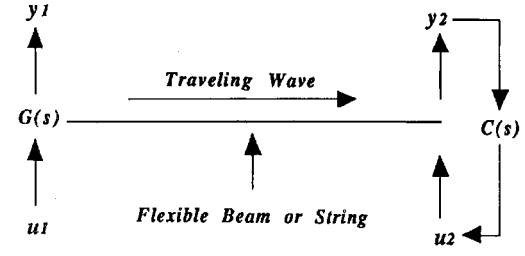

Fig. 6 Sensor and actuator location for dereverberated system.

$$G_{01} = Q^{-1}G_{10}Q, \qquad G_{00} = Q^{-1}G_{11}Q, \qquad Q = \begin{bmatrix} 1 & 0 \\ 0 & -1 \end{bmatrix} \tag{32}$$

where $y = [\dot{w}\dot{\theta}]^T$ are sensor outputs and $u = [MF]^T$ the controller inputs; the subscripts 0 and 1 denote the left and right ends of the beam, respectively, and each G_{ij} is a transfer function between the output y_i and input u_j. The algebraic manipulation using Eqs. (30) and (31) with $u_1 = -X_0 y_1$ to cancel all of the reflective waves at the right end yields the closed-loop transfer function at the left end

$$X_0 = G_{00} - G_{01}X_0(I + G_{11}X_0)^{-1}G_{10} \tag{33}$$

The problem is to find the compensator that is identical to the closed-loop transfer function. The solution to Eq. (33) is analyzed with finite dimensions in the next section.

Analysis of the Solution in Finite Dimensions

The analysis of the solution to Eq. (33) proceeds in a way similar to the exact model-matching problem.[15] The problem is to find a dynamic compensator to achieve a given closed-loop response, and it only differs from the present case in that a prefilter is also employed to replace the invariant zeros of the open-loop plant with those of the desired closed-loop, in addition to the feedback into the system.

The closed-loop transfer function in Eq. (33) can also be represented as follows:

$$\begin{aligned} X_0 &= G_{00} - G_{01}X_0(I + G_{11}X_0)^{-1}G_{10} \\ &= G_{00} - G_{01}X_0Z_0 \end{aligned} \tag{34}$$

where

$$Z_0 \equiv (I + G_{11}X_0)^{-1}G_{10} \tag{35}$$

Using the symmetrical properties for the sensor and actuator locations, similar relations hold for Z_0

$$\begin{aligned} Z_0 &= G_{10} - G_{11}Z_0(I + G_{01}Z_0)^{-1}G_{00} \\ &= G_{10} - G_{11}Z_0X_0 \end{aligned} \tag{36}$$

and

$$X_0 = (I + G_{01}Z_0)^{-1}G_{00} \tag{37}$$

The transfer function Z_0 has the same closed-loop poles as those of X_0, and it is also a DTF with a nonminimum phase. The sensor outputs at the left end are fedback into the controller inputs at the right end to cancel all of the reflective waves in this case. The right side of Eq. (33) is such a complex structure that Eqs. (35) and (37) are analyzed in a way similar to the exact model matching problem in place of Eq. (33).

Introducing a matrix-fraction description[16] for each transfer function

$$X_0 = F_L^{-1}G_L = G_R F_R^{-1}, \qquad Z_0 = P_L^{-1}Q_L = Q_R P_R^{-1} \tag{38}$$

$$\begin{aligned} G_{00} &= A^{-1}B_0, & G_{11} &= A^{-1}\tilde{B}_0 \\ G_{01} &= A^{-1}B_1, & G_{10} &= A^{-1}\tilde{B}_1 \end{aligned} \tag{39}$$

where the DTFs are assumed to be expressed in a matrix-fraction description, as shown in Eq. (38), and A and each B_i are left coprime polynomial matrices with $\det A \neq 0$ in Eq. (39).

Substitution of Eqs. (38) and (39) into Eq. (37) gives

$$P_R(AP_R + B_1Q_R)^{-1}B_0 = G_R F_R^{-1} \tag{40}$$

and

$$P_R(AP_R + B_1Q_R)^{-1}B_0F_R = G_R \tag{41}$$

where use has been made of the right matrix-fraction descriptions of Eq. (38) in the preceding computations. It can be easily shown that the relations

$$AP_R + B_1 Q_R = TP_R \tag{42}$$

$$TG_R = B_0 F_R \tag{43}$$

satisfy Eq. (41) for an arbitrary invertible polynomial matrix T. Equation (43) may be rewritten with the help of Eq. (38) as

$$T^{-1}B_0 = G_R F_R^{-1} = F_L^{-1} G_L \tag{44}$$

From Eq. (44) we obtain

$$F_L = T, \qquad G_L = B_0 \tag{45}$$

where the second equation of Eq. (45) reflects the well-known fact that zeros of an open-loop plant are invariant under any feedback into the system. An analogous argument applies to Eq. (35) and the results are

$$AF_R + \tilde{B}_0 G_R = \tilde{T} F_R \tag{46}$$

$$\tilde{T} Q_R = \tilde{B}_1 P_R \tag{47}$$

and

$$P_L = \tilde{T}, \qquad Q_L = \tilde{B}_1 \tag{48}$$

Making use of Eqs. (45) and (48), Eqs. (42) and (46) become

$$A + B_1 \tilde{T}^{-1} \tilde{B}_1 = T \tag{49}$$

$$A + \tilde{B}_0 T^{-1} B_0 = \tilde{T} \tag{50}$$

Thus, solving of the problem has been reduced to finding T and $\tilde{T}$ from Eqs. (49) and (50). The approximate solutions can be obtained through the use of the least-squares procedure in a manner similar to the preceding sections, which leads to a nonlinear optimization problem. No initial guess is found to the optimal solutions in the present case. Exact solutions are used to reduce the problem to the linear optimization problem, that is, Eqs. (49) and (50) are replaced by

$$A + B_1 Z_0 = T \tag{51}$$

and

$$A + \tilde{B}_0 X_0 = \tilde{T} \tag{52}$$

where the exact solutions, X_0 and Z_0, are expressed by an irrational function,

$$X_0 = \begin{bmatrix} 1 & 1/q \\ -2q & -1 \end{bmatrix}$$

$$Z_0 = e^{-q} \begin{bmatrix} \cos q - \sin q & \cos q/q \\ -2q \cos q & -\cos q - \sin q \end{bmatrix} \tag{53}$$

where $q = \sqrt{(s/2)}$. The second terms of the left-hand side of Eqs. (51) and (52), $B_1 Z_0$ and $\tilde{B}_0 X_0$, are fitted with the models $\hat{y}(s)$ in the form

$$\hat{y}(s) = \sum_{n=0}^{M} a_n P_n(s) \tag{54}$$

where each a_n is to be determined and $P_n(s)$ is the nth-order polynomial with an orthogonal relation

$$\sum_{i=1}^{N} |y(s_i)|^{-2} Re\left[P_n(s_i) P_k^*(s_i)\right] = 0 \qquad n \neq k \tag{55}$$

where the cost is defined as

$$J = \sum_{i=1}^{N} |y(s_i)|^{-2} |\hat{y}(s_i) - y(s_i)|^2 \tag{56}$$

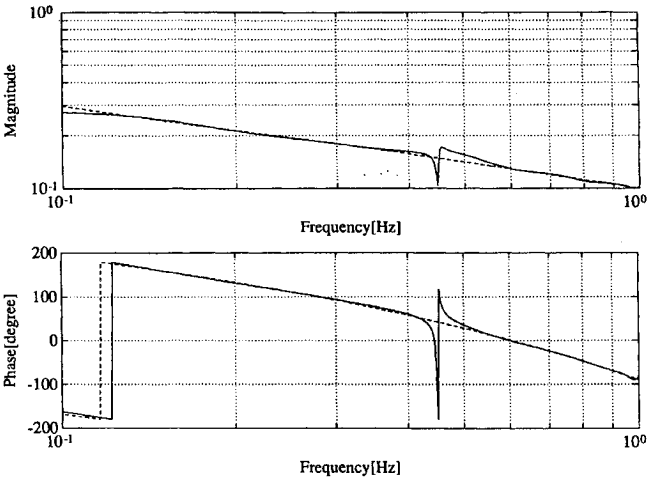

Fig. 7 Comparison of the optimal approximation (solid line) with the ideal (dashed line) for (1,2) element of Z_0.

and where y is the exact value of the elements of $B_1 Z_0$ and $\tilde{B}_0 X_0$ and it is computed with the help of Eq. (53). Each a_n is determined by making use of the inner products between the orthogonal polynomials in a standard manner and as the results the DTFs X_0 and Z_0 are represented by a polynomial matrix in finite dimensions. Figure 7 shows comparison of the approximate DTF with the ideal for $(1,2)$ element of Z_0, by which other elements are qualitatively represented, including those of X_0. A perfect pole-zero cancelation would lead to good agreement between the ideal and approximate DTFs. Better approximations are required in the least-squares procedures, as shown in Fig. 7. Larger model order theoretically gives the better approximations with a sufficient number of the sampled points in the least-squares procedures: Numerical difficulties are encountered due to lack of the orthogonalities in the polynomials higher than 21st order. The evaluated points are sampled over the range from 0.8 to 8 Hz with only a flexible mode; this range is normalized to the range between 0.1 and 1 Hz in the numerical procedures. No lower cost is obtained in the least-squares procedure for the models higher than 21st order. A significantly higher order polynomial is required in the denominator than in the numerator for the DTF in the present case.

Conclusion

The DTF is well approximated by making use of the model based on the RTF with damping augmentation. In a spring-mass system, the DTF is derived from the equation of motion to be of discontinuous slope and of infinite dimensions, whereas the RTF of finite dimensions. Another approximate expression is obtained for the DTF derived from the fact that the closed-loop transfer function is identical to the DTF when all of the reflective waves are canceled at the structural boundaries except for the location of the actuators. The DTF is represented as a solution of an algebraic equation with frequency-varying coefficients. On making use of a matrix-fraction description, the problem leads to solving a nonlinear equation with respect to the polynomial matrices. The approximate solution is obtained with the help of the least-squares procedures for model fitting based on the orthogonal polynomials. A perfect pole-zero cancelation is not achieved to give disagreement between the ideal and approximated DTFs due to the numerical difficulties for lack of the orthogonalities on the polynomials.

References

[1]Skudrzyk, E., "The Mean-Value Method of Predicting the Dynamic Response of Complex Vibrators," *Journal of the Acoustical Society of America*, Vol. 67, No. 4, 1980, pp. 1105–1135.

[2]Vaughan, D. R., "Application of Distributed Parameter Concepts to Dynamical Analysis and Control of Bending Vibrations," *Journal of Basic Engineering*, June 1968, pp. 157–166.

[3]von Flotow, A. H., and Schäfer, B., "Wave-Absorbing Controllers for a Flexible Beam," *Journal of Guidance, Control, and Dynamics*, Vol. 9, No. 6, 1986, pp. 673–680.

[4]Miller, D. W., and Hall, S. R., "Experimental Results Using Active Control of Traveling Wave Power Flow," *Journal of Guidance, Control, and Dynamics*, Vol. 14, No. 2, 1991, pp. 350–359.

[5]Mace, B. R., "Active Control of Flexural Vibrations," *Journal of Sound and Vibration*, Vol. 114, No. 2, 1987, pp. 253–270.

[6]Fujii, H., Ohtsuka, T., and Murayama, T., "Wave-Absorbing Control for Flexible Structures with Non-Collocated Sensors and Actuators," *Journal of Guidance, Control, and Dynamics*, Vol. 15, No. 2, 1992, pp. 431–439.

[7]MacMartin, D. G., and Hall, S. R., "Control of Uncertain Structures Using an H_∞ Power Flow Approach," *Journal of Guidance, Control, and Dynamics*, Vol. 14, No. 3, 1991, pp. 521–530.

[8]MacMartin, D. G., and Hall, S. R., "A Stochastic Approach to Broadband Control of Parametrically Uncertain Structures," Massachusetts Inst. of Technology Space Engineering Research Center, Cambridge, MA, May 1992.

[9]Gu, G., Khargonekar, P. P., and Bruce, E., "Approximation and Infinite-Dimensional Systems," *IEEE Transactions on Automatic Control*, Vol. 34, No. 6, 1989, pp. 610–618.

[10]Wu, N. E., and Gu, G., "Discrete Fourier Transform and H_∞ Approximation," *IEEE Transactions on Automatic Control*, Vol. 35, No. 9, pp. 1044–1046.

[11]Glover, K., Curtain, R. F., and Partington, J. R., "Realization and Approximation of Linear Infinite-Dimensional Systems with Error Bounds," *Journal of Control and Optimization*, Vol. 26, No. 4, 1988, pp. 863–871.

[12]Matsuda, K., and Fujii, H., "On the Matched Termination for Vibration Suppression," *Proceedings of the AIAA Guidance, Navigation, and Control Conference* (Baltimore, MD), AIAA, Washington, DC, 1995, pp. 112–121.

[13]Sidman, M. D., DeAngelis, F. E., and Verghese, G. C., "Parametric System Identification on Logarithmic Frequency Response Data," *IEEE Transactions on Automatic Control*, Vol. 36, No. 9, 1991, pp. 1065–1070.

[14]Miu, D. K., "Physical Interpretation of Transfer Function Zeros for Simple Control Systems with Mechanical Flexibilities," *Journal of Dynamic Systems, Measurement, and Control*, Vol. 113, Sept. 1989, pp. 419–424.

[15]Kaczorek, T., "Polynomial Equation Approach to Exact Model Matching Problem in Multivariable Linear Systems," *International Journal of Control*, Vol. 36, No. 3, 1982, pp. 531–539.

[16]Kailath T., *Linear Systems*, Prentice–Hall, Englewood Cliffs, NJ, 1980, Chap. 6.